DALTON

$[HN(CH_2CH_2)_3NH]_3[Fe_8(HPO_4)_{12}(PO_4)_2(H_2O)_6]$: an organically templated iron phosphate with a pillared layer structure

Kwang-Hwa Lii* and Yuh-Feng Huang

Institute of Chemistry, Academia Sinica, Taipei, Taiwan

An organically templated iron phosphate, $[HN(CH_2CH_2)_3NH]_3[Fe_8(HPO_4)_{12}(PO_4)_2(H_2O)_6]$, has been synthesized under solvothermal conditions and characterized by single-crystal X-ray diffraction, Mössbauer spectroscopy and thermogravimetric analysis. The compound crystallizes in the trigonal space group $P\bar{3}c1$ (no. 165) with $a = 13.5274(5)$, $c = 19.2645(6)$ Å, $U = 3052.9(3)$ Å^3 and $Z = 2$. The structure consists of layers of corner-sharing FeO_6 and $FeO_5(OH_2)$ octahedra and PO_4 and $PO_3(OH)$ tetrahedra which are pillared through additional FeO_6 octahedra to form a three-dimensional framework structure. The framework contains a two-dimensional array of intersecting channels in which the charge compensating diprotonated 1,4-diazabicyclo[2.2.2]octane cations reside. The framework is closely related to that of an imidazole encapsulating indium phosphate, $[H_3O][C_3N_2H_5]_3[In_8(HPO_4)_{14}(H_2O)_6]\cdot 5H_2O$.

Recently we have synthesized a large number of ternary iron phosphates by high temperature, high pressure hydrothermal methods. These compounds present a variety of complex crystal structures and thus interesting magnetic properties and are a challenge to complete characterization. Their structures cover discrete FeO_6 octahedra, FeO_5 trigonal bipyramids, dimers of corner-sharing, edge-sharing or face-sharing FeO_6 octahedra, trimeric, tetrameric units of Fe–O polyhedra and infinite chains of FeO_6 octahedra sharing either *trans* or skew edges. They include iron(II), iron(III) and mixed-valence compounds.[1] However, syntheses performed under high temperature, high pressure hydrothermal conditions can only yield dense phases. To generate large internal micropore volumes within the inorganic oxide frameworks, the syntheses are usually carried out under mild hydrothermal conditions (<200 °C) with a variety of organic cationic templates. Some of the microporous materials were synthesized from predominantly non-aqueous systems. Recently, an organically templated iron phosphate $[H_3NCH_2CH_2NH_3]_{0.5}[Fe(OH)(PO_4)]$ was reported.[2,3] It adopts a layered structure with the ethylenediammonium cations in the interlayer region, which is isotypic with the layered gallophosphate obtained in ethylene glycol ($HOCH_2CH_2OH$).[4] A fluorinated iron phosphate with an open structure, $[C_6H_{14}N_2][Fe_4(PO_4)_4F_2(H_2O)_3]$ was reported recently.[5] The framework consists of large cages limited by three-, four-, six- and eight-membered windows in which the diprotonated 1,4-diazabicyclo[2.2.2]octane cations are located. We have also become interested in the synthesis of microporous metal phosphates under mild solvothermal conditions because of their rich structural chemistry and potential applications as molecular sieves, ion-exchange materials and catalysts. Here we describe the solvothermal synthesis and characterization of a 1,4-diazabicyclo[2.2.2]octane encapsulating iron phosphate, $[HN(CH_2CH_2)_3NH]_3[Fe_8(HPO_4)_{12}(PO_4)_2(H_2O)_6]$, which exhibits a pillared layer structure. Its inorganic oxide framework is closely related to that of an indium phosphate with encapsulated imidazolium cation as the template, $[H_3O][C_3N_2H_5]_3[In_8(HPO_4)_{14}(H_2O)_6]\cdot 5H_2O$.[6]

Experimental

Synthesis and initial characterization

The synthesis was carried out in a Teflon-lined acid digestion bomb (23 cm^3) under autogenous pressure. The reaction of $FeCl_3\cdot 6H_2O$ (2.5 mmol), 1,4-diazabicyclo[2.2.2]octane (DABCO) (7.5 mmol), H_3PO_4 (7.5 mmol), *n*-butanol (3 cm^3) and water (7 cm^3) at 180 °C for 3 d followed by slow cooling at 10 °C h^{-1} to room temperature produced $[HN(CH_2CH_2)_3NH]_3[Fe_8(HPO_4)_{12}(PO_4)_2(H_2O)_6]$ **1** as colourless crystals and a small amount of a green material. The colourless crystals were manually separated from the green material to give pure compound **1** as judged by visual microscopic examination and by comparison of the X-ray powder pattern to the pattern simulated from the atomic coordinates derived from a single-crystal study. The yield was 70% based on iron. Energy-dispersive X-ray fluorescence analysis using a JEOL analytical electron microscope confirmed the presence of Fe and P but no Cl in the colourless crystals {Found: C, 9.60; H, 2.98; N, 3.73%. Calc. for $[HN(CH_2CH_2)_3NH]_3[Fe_8(HPO_4)_{12}(PO_4)_2(H_2O)_6]$: C, 9.66; H, 2.97; N, 3.75%, confirming that 1,4-diazabicyclo[2.2.2]octane is present in the compound}. The pure sample was used for thermogravimetric analysis and Mössbauer spectroscopy measurements.

Thermogravimetric analysis of **1** was performed on a Perkin-Elmer TGA7 thermal analyser: the sample was heated to 950 °C at 10 °C min^{-1} in air. In order to characterize the decomposition products, an experiment was performed in which **1** was heated at 325, 400, 600 and 800 °C for 8 h in a platinum crucible in air. The product of each heat treatment was analysed by powder X-ray diffraction at room temperature. The ^{57}Fe Mössbauer measurements were made on a constant-acceleration instrument at 300 K. Isomer shift is reported with respect to an iron foil standard.

Single-crystal X-ray diffraction

Most of the colourless crystals were not suitable for single-crystal X-ray structure analysis as indicated from peak profile analysis. Many were selected before a satisfactory crystal was obtained. A small tabular crystal of dimensions 0.1 × 0.1 × 0.025 mm was mounted on a Siemens Smart-CCD diffractometer equipped with a normal focus, 3 kW sealed tube X-ray source. Intensity data were collected in 1200 frames with increasing ω (width of 0.3° per frame). The orientation matrix and unit cell dimensions were determined by a least-squares fit of 4881 reflections with $2.5 < 2\theta < 50°$. Absorption correction was based on 4356 symmetry-equivalent reflections using the SHELXTL PC program package (T_{min}, $T_{max} = 0.751$, 0.884).[7] On the basis of systematic absences, statistical analysis of the

* E-Mail: lii@chem.sinica.edu.tw

Table 1 Crystallographic data for $[HN(CH_2CH_2)_3NH]_3[Fe_8(HPO_4)_{12}(PO_4)_2(H_2O)_6]$

Formula	$C_{18}Fe_8H_{66}N_6O_{62}P_{14}$
M	2239.15
Crystal system	trigonal
Space group	$P\bar{3}c1$
a/Å	13.5274(5)
c/Å	19.2645(6)
U/Å^3	3052.9(3)
Z	2
D_c/g cm^{-3}	2.436
$F(000)$	2260
μ(Mo-Kα)/cm^{-1}	23.6
T/°C	23
λ/Å	0.710 73
Maximum 2θ/°	53.5
Reflections collected	17 333
Unique reflections	2516
Observed unique reflections [$I > 3\sigma(I)$]	1335
Weighting scheme	$w^{-1} = \sigma^2(F) + 0.000\,322F^2$
Number of parameters	165
R_{int}	0.0760
R_F [a]	0.0634
R' [b]	0.0589
Goodness of fit	1.90
$(\Delta\rho)_{max,min}$/e Å^{-3}	0.92, −0.84

[a] $R = \Sigma||F_o| - |F_c||/\Sigma|F_o|$. [b] $R' = [\Sigma w(|F_o| - |F_c|)^2/\Sigma w|F_o|^2]^{\frac{1}{2}}$.

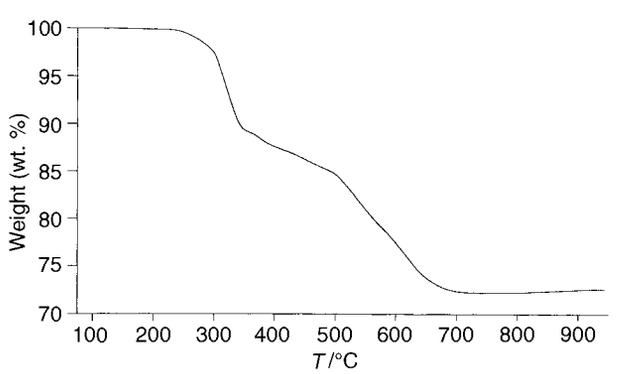

Fig. 1 Thermogravimetric analysis of $[HN(CH_2CH_2)_3NH]_3[Fe_8(HPO_4)_{12}(PO_4)_2(H_2O)_6]$ in flowing air at 10 °C min^{-1}

intensity distribution, and successful solution and refinement of the structure, the space group was determined to be $P\bar{3}c1$ (no. 165). The structure was solved by direct methods: the iron and phosphorus atoms were first located and the oxygen, carbon and nitrogen atoms were found in Fourier-difference maps. The hydrogen atoms were not located. Bond-valence calculations[8] indicated that O(2), O(6), O(9) and O(11) had valence sums of 1.10, 1.09, 1.18 and 0.36, respectively, and all other oxygen atoms had values between 1.75 and 1.93. The value 0.36 indicates that O(11) is a water oxygen. Two more hydrogen atoms at general positions must be included to balance the charge. Valence sums of 1.10 and 1.09 suggest that O(2) and O(6) are hydroxo oxygens. Atom O(9) sits on a three-fold axis and is hydrogen bonded to three DABCO cations with the O···N distances at 2.78 Å. The final cycles of least-squares refinement on F including atomic coordinates and anisotropic thermal parameters for all atoms converged at $R = 0.0634$ and $R' = 0.0589$. The final Fourier-difference maps were flat to $(\Delta\rho)_{max,min} = 0.92, -0.84$ e Å^{-3}. Neutral-atom scattering factors were used for all atoms. Anomalous dispersion and secondary extinction corrections were applied. Structure solution and refinement were performed on SHELXTL PC programs.

Atomic coordinates, thermal parameters, and bond lengths and angles have been deposited at the Cambridge Crystallographic Data Centre (CCDC). See Instructions for Authors, *J. Chem. Soc., Dalton Trans.*, 1997, Issue 1. Any request to the CCDC for this material should quote the full literature citation and the reference number 186/520.

Table 2 Atomic coordinates for $[HN(CH_2CH_2)_3NH]_3[Fe_8(HPO_4)_{12}(PO_4)_2(H_2O)_6]$

Atom	x	y	z
Fe(1)	0.855 6(1)	0.565 5(1)	0.450 37(7)
Fe(2)	0	0	0.25
Fe(3)	0	0	0.5
P(1)	0.963 5(2)	0.812 1(2)	0.371 2(1)
P(2)	0.632 1(2)	0.505 1(2)	0.543 9(1)
P(3)	0.666 7	0.333 3	0.362 5(2)
O(1)	0.880 9(5)	0.686 0(5)	0.383 1(3)
O(2)	0.081 2(6)	0.824 9(6)	0.347 5(4)
O(3)	0.923 4(6)	0.859 7(5)	0.312 8(3)
O(4)	0.983 6(9)	0.874 8(7)	0.440 2(3)
O(5)	0.713 5(5)	0.564 1(5)	0.483 7(3)
O(6)	0.702 5(5)	0.495 0(6)	0.606 6(3)
O(7)	0.580 0(5)	0.574 1(5)	0.571 1(3)
O(8)	0.542 8(6)	0.382 0(5)	0.527 3(3)
O(9)	0.666 7	0.333 3	0.281 8(5)
O(10)	0.772 2(5)	0.443 2(5)	0.386 2(3)
O(11)	0.939 0(5)	0.691 7(5)	0.529 3(3)
N(1)	0.602 9(8)	0.496 2(8)	0.257 7(4)
C(1)	0.625 8(9)	0.571 2(9)	0.318 9(5)
C(2)	0.476 4(9)	0.411 7(9)	0.252 8(6)
C(3)	0.645(1)	0.569(1)	0.192 5(6)

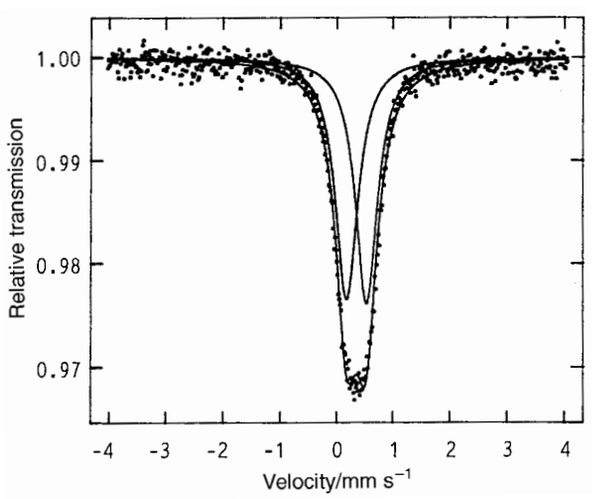

Fig. 2 Mössbauer spectrum of $[HN(CH_2CH_2)_3NH]_3[Fe_8(HPO_4)_{12}(PO_4)_2(H_2O)_6]$ at 300 K

Results and Discussion

Physical measurements

The TG analysis showed weight loss in three steps (Fig. 1). The step in the temperature range from ≈350 to ≈500 °C is not resolved from the other two steps. On the basis of powder X-ray analysis, the decomposition products at 325, 400 and 600 °C are amorphous. The product at 800 °C is a mixture of $Fe_4(P_2O_7)_3$ and $Fe(PO_3)_3$.† At present we are unable to rationalize the decomposition mechanism of each step. The observed total weight loss of 27.7% between room temperature and 800 °C agrees well with that calculated for the loss of 15 H_2O and 3 DABCO molecules (27.1%), as indicated from equation (1).

$$[HN(CH_2CH_2)_3NH]_3[Fe_8(HPO_4)_{12}(PO_4)_2(H_2O)_6] \longrightarrow Fe_4(P_2O_7)_3 + 8/3\ Fe(PO_3)_3 + 2/3\ Fe_2O_3 + 15\ H_2O + 3\ N(CH_2CH_2)_3N \quad (1)$$

† $Fe_4(P_2O_7)_3$, file number 36-318; $Fe(PO_3)_3$, 38-109; Joint Committee on Powder Diffraction Standards, International Center of Diffraction Data, Swarthmore, PA.

Table 3 Interatomic distances and bond valence sums (Σ*s*) for $[HN(CH_2CH_2)_3NH]_3[Fe_8(HPO_4)_{12}(PO_4)_2(H_2O)_6]$

$Fe(1)O_6$ octahedron*

Fe(1)	O(1)	O(5)	O(10)	O(11)	O(7a)	O(8a)
O(1)	**1.973(7)**	2.806(8)	2.850(9)	2.915(9)	2.849(9)	
O(5)	89.4(3)	**2.016(8)**	2.852(10)	2.790(8)		2.853(8)
O(10)	94.2(3)	92.9(3)	**1.916(6)**		2.871(9)	2.841(9)
O(11)	90.2(3)	84.3(3)	174.8(2)	**2.138(6)**	2.865(9)	2.758(9)
O(7a)	92.0(3)	172.1(2)	94.7(3)	87.9(3)	**1.987(4)**	2.774(11)
O(8a)	173.3(3)	90.0(2)	92.5(3)	83.1(3)	87.7(2)	**2.017(6)**

Σ*s*[Fe(1)–O] = 3.11

$Fe(2)O_6$ octahedron*

Fe(2)	O(3a)	O(3b)	O(3c)	O(3d)	O(3e)	O(3f)
O(3a)	**2.042(6)**	2.851(7)		3.011(12)	2.843(14)	2.851(7)
O(3b)	88.5(2)	**2.042(6)**	3.011(12)	2.843(14)		2.851(7)
O(3c)	88.5(2)	88.5(2)	**2.042(3)**	2.851(7)	2.851(7)	2.843(14)
O(3d)	88.2(4)	175.1(4)	95.0(4)	**2.042(6)**	2.851(7)	
O(3e)	175.1(4)	95.0(4)	88.2(4)	88.5(2)	**2.042(6)**	3.011(12)
O(3f)	95.0(4)	88.2(4)	175.1(4)	88.5(2)	88.5(2)	**2.042(3)**

Σ*s*[Fe(2)–O] = 2.79

$Fe(3)O_6$ octahedron*

Fe(3)	O(4a)	O(4b)	O(4c)	O(4d)	O(4e)	O(4f)
O(4a)	**1.967(9)**	2.802(12)	2.761(12)	2.802(12)	2.761(12)	
O(4b)	180.0(0)	**1.967(9)**		2.761(12)	2.802(12)	2.761(12)
O(4c)	89.2(2)	90.8(2)	**1.967(7)**	2.802(12)	2.761(12)	2.802(12)
O(4d)	90.8(2)	89.2(2)	180.0(0)	**1.967(7)**		2.761(12)
O(4e)	89.2(2)	90.8(2)	89.2(2)	90.8(2)	**1.967(5)**	2.802(12)
O(4f)	90.8(2)	89.2(2)	90.8(2)	89.2(2)	180.0(0)	**1.967(5)**

Σ*s*[Fe(3)–O] = 3.42

$P(1)O_4$ tetrahedron

P(1)	O(1)	O(2)	O(3)	O(4)
O(1)	**1.518(6)**	2.500(8)	2.517(10)	2.473(9)
O(2)	107.6(5)	**1.581(9)**	2.496(13)	2.506(14)
O(3)	111.7(4)	107.0(4)	**1.524(8)**	2.562(9)
O(4)	108.6(4)	107.5(5)	114.2(6)	**1.527(8)**

Σ*s*[P(1)–O] = 4.97

$P(2)O_4$ tetrahedron

P(2)	O(5)	O(6)	O(7)	O(8)
O(5)	**1.521(6)**	2.522(9)	2.522(10)	2.533(7)
O(6)	108.5(4)	**1.585(8)**	2.475(12)	2.456(8)
O(7)	112.2(4)	105.9(4)	**1.516(9)**	2.532(10)
O(8)	112.5(4)	104.4(4)	112.8(4)	**1.524(6)**

Σ*s*[P(2)–O] = 4.99

$P(3)O_4$ tetrahedron

P(3)	O(9)	O(10)	O(10a)	O(10b)
O(9)	**1.556(11)**	2.484(10)	2.484(10)	2.484(10)
O(10)	107.4(3)	**1.528(5)**	2.525(8)	2.525(8)
O(10a)	107.4(3)	111.5(3)	**1.528(8)**	2.525(8)
O(10b)	107.4(3)	111.5(3)	111.5(2)	**1.528(4)**

Σ*s*[P(3)–O] = 5.00

$[HN(CH_2CH_2)_3NH]^{2+}$ cation

N(1)–C(1)	1.48(1)	N(1)–C(2)	1.51(1)
N(1)–C(3)	1.52(1)	C(1)–C(3a)	1.54(2)
C(2)–C(2a)	1.52(3)		
C(1)–N(1)–C(2)	109.6(9)	C(1)–N(1)–C(3)	109.2(9)
C(2)–N(1)–C(3)	110.7(9)	N(1)–C(1)–C(3a)	109.0(9)
N(1)–C(2)–C(2a)	109.2(7)	N(1)–C(3)–C(1a)	108.5(10)
O(9)···N(1)	2.78(1) (3×)		

* The distances between *trans* oxygen atoms are not shown.

The room-temperature Mössbauer spectrum of **1** (Fig. 2) can be least-squares fitted by one doublet and does not show three Fe components as observed in the crystal structure. The obtained parameters are δ (isomer shift) = 0.45 mm s^{-1}, ΔE_Q (quadrupole splitting) = 0.35 mm s^{-1} and Γ (full width at half-height) = 0.47 mm s^{-1}. The peaks are broader than those for a thin iron calibration foil (Γ = 0.30 mm s^{-1}). The isomer shift is characteristic of high-spin Fe^{III}. According to Menil,[9] the usual ranges of isomer shifts in oxides are 0.29–0.50 and 1.03–1.28 mm s^{-1} for Fe^{III} and Fe^{II} in six-co-ordination, respectively. Therefore, the composition of **1** is further defined by Mössbauer spectroscopy and TG analysis.

Crystal structure

The crystallographic data are listed in Table 1. Atomic coordinates, interatomic distances, bond angles and bond-valence sums are given in Tables 2 and 3, respectively. The iron atoms Fe(2) and Fe(3) are at special positions with local symmetries D_3 and S_6, respectively. The atoms P(3) and O(9) sit on three-fold axes and all other atoms are at general positions. The Fe and P atoms are six- and four-co-ordinate, respectively. Both the $Fe(2)O_6$ and $Fe(3)O_6$ octahedra are quite regular. The $Fe(1)O_6$ octahedron is considerably more distorted. The Fe(1)–O(11) distance is the longest because O(11) is the water oxygen. The

Fe(2)–O distances are significantly longer than those of Fe(3)–O. Both P(1) and P(2) have a terminal P–OH group as shown by the unsatisfied valence sums for O(2) and O(6) and the longer P–O distances [P(1)–O(2) 1.581 and P(2)–O(6) 1.585 Å]. The P(3)–O(9) distance is also longer at 1.556 Å. The valence sum of O(9) is satisfied by forming three O · · · H–N bonds with three different protonated DABCO cations. In the indium phosphate $[H_3O][C_3N_2H_5]_3[In_8(HPO_4)_{14}(H_2O)_6]\cdot 5H_2O$ all three distinct phosphorus atoms form hydrogen phosphate groups.

The structure of $[HN(CH_2CH_2)_3NH]_3[Fe_8(HPO_4)_{12}(PO_4)_2(H_2O)_6]$, viewed along the [100] direction, is shown in Fig. 3. It consists of macroanionic sheets normal to [001], in which the $Fe(3)O_6$ and $Fe(1)O_5(OH_2)$ octahedra share corners with the PO_4 and $PO_3(OH)$ tetrahedra in an alternating manner to form four- and six-membered rings (Fig. 4). The connectivity is the same as that in $[H_3O][C_3N_2H_5]_3[In_8(HPO_4)_{14}(H_2O)_6]\cdot 5H_2O$. The sheets are linked through $Fe(2)O_6$ pillars to generate intersecting channels parallel to the ⟨100⟩ directions in which the diprotonated DABCO cations reside. Within the channels are 14-membered rings formed by seven iron–oxygen octahedra and seven phosphate tetrahedra (Fig. 5). The terminal P(3)–O(9) groups are directed towards the interlayer region and receive three hydrogen bonds from neighbouring DABCO cations. Intralayer hydrogen bonds also exist as inferred from the O · · · O distances. In the indium compound the channels contain positionally disordered imidazolium cations and water molecules. One-sixth of the non-framework water molecules are protonated to achieve charge balance with the framework.

The compound described here is a second example of an organic molecule encapsulated open-framework structure of iron phosphate. Its inorganic oxide framework is similar to that of an indium phosphate. It provides another example of a large class of metastable phases of open-framework structures which may be accessible within hydrothermal reaction domains. The introduction of different organic templates into the Fe–P–O system leads to different structures which are very sensitive not only to the nature of the templates incorporated but also to reaction conditions. Other hydrothermally prepared iron phosphates with open-framework structures have been prepared and will be presented in future publications.

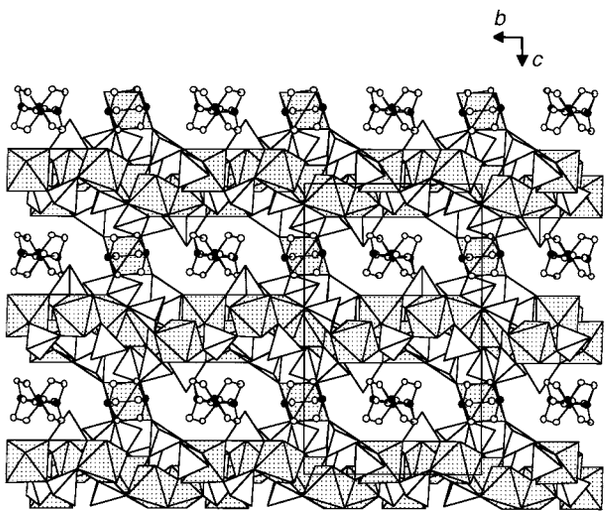

Fig. 3 Polyhedral representation of the $[HN(CH_2CH_2)_3NH]_3[Fe_8(HPO_4)_{12}(PO_4)_2(H_2O)_6]$ structure viewed along the *a* axis. Open circles, C atoms; solid circles, N atoms

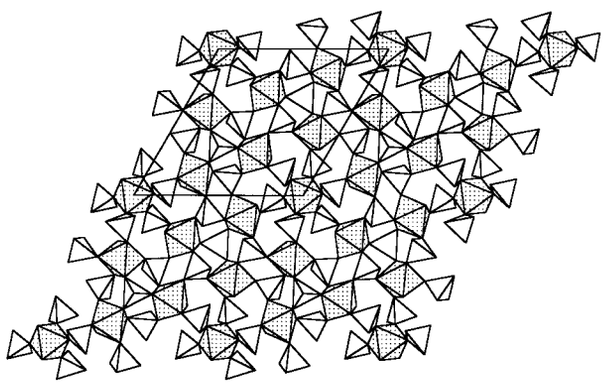

Fig. 4 A layer of the $[HN(CH_2CH_2)_3NH]_3[Fe_8(HPO_4)_{12}(PO_4)_2(H_2O)_6]$ structure viewed along the *c* axis

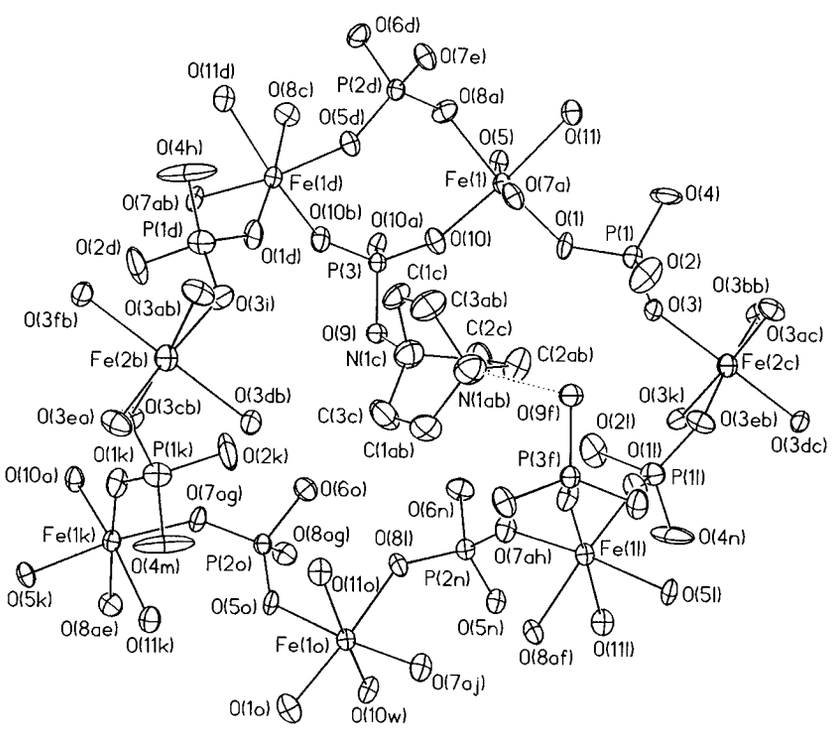

Fig. 5 A 14-membered ring containing a diprotonated 1,4-diazabicyclo[2.2.2]octane cation viewed along the *a* axis. Hydrogen-bonding interactions, O(9) · · · H–N, are shown as dotted lines. Thermal ellipsoids are shown at 50% probability

Acknowledgements

We thank the Institute of Chemistry, Academia Sinica and the National Science Council (NSC86-2113-M-001-014) for support, Professor S.-L. Wang and Ms. F.-L. Liao at the National Tsing Hua University for X-ray intensity data collection, and Professor T.-Y. Dong at the National Sun Yat-Sen University for Mössbauer spectroscopy measurements.

References

1 K.-H. Lii, T.-Y. Dong, C.-Y. Cheng and S.-L. Wang, *J. Chem. Soc., Dalton Trans.*, 1993, 577; K.-H. Lii, P.-F. Shih and T.-M. Chen, *Inorg. Chem.*, 1993, **32**, 4373; E. Dvoncova and K.-H. Lii, *Inorg. Chem.*, 1993, **32**, 4368; K.-H. Lii, *J. Chem. Soc., Dalton Trans.*, 1994, 931; K.-H. Lii and C.-Y. Huang, *J. Chem. Soc., Dalton Trans.*, 1995, 571; *Eur. J. Solid State Inorg. Chem.*, 1995, **32**, 225; K.-H. Lii, *Eur. J. Solid State Inorg. Chem.*, 1995, **32**, 225; K.-H. Lii, *J. Chem. Soc., Dalton Trans.*, 1996, 819.

2 M. Cavellec, D. Riou and G. Ferey, *Acta Crystallogr., Sect. C*, 1995, **51**, 2242.

3 J. R. D. DeBord, W. M. Reiff, R. C. Haushalter and J. Zubieta, *J. Solid State Chem.*, 1996, **125**, 185.

4 R. H. Jones, J. M. Thomas, H. Qisheng, R. Xu, M. B. Hursthouse and J. Chen, *J. Chem. Soc., Chem. Commun.*, 1991, 150.

5 M. Cavellec, D. Riou, C. Ninclaus, J.-M. Greneche and G. Ferey, *Zeolites*, 1996, **17**, 250.

6 A. M. Chippindale, S. J. Brech, A. R. Cowley and W. M. Simpson, *Chem. Mater.*, 1996, **8**, 2259.

7 G. M. Sheldrick, SHELXTL PC, Version 5, Siemens Analytical X-Ray Instruments Inc., Madison, WI, 1995.

8 I. D. Brown and D. Altermatt, *Acta Crystallogr., Sect. B*, 1985, **41**, 244.

9 F. Menil, *J. Phys. Chem. Solids*, 1985, **46**, 763.

Received 21*st January* 1997; *Paper* 7/00472I